

## Phase relation between phase locked (2,1) and (3,1) tearing modes in ASDEX Upgrade

A. Gude, M. Maraschek, V. Igochine, M. Willensdorfer, H. Zohm, ASDEX Upgrade Team  
 Max Planck Institute for Plasma Physics, D-85748 Garching, Germany

**Introduction** Tearing modes (TMs) are a major concern for tokamak operation. Especially an ( $m = 2, n = 1$ ) TM (with  $m$  poloidal and  $n$  toroidal mode number) can lead to strong confinement reduction and also trigger a disruption when locking, i.e. getting stationary with respect to the vacuum vessel. Reliably detecting rotating or locked (2,1) modes is therefore necessary in order to initiate countermeasures. Rotating tearing modes can be detected by spatially filtered signals from sets of magnetic pick-up coils, often in combination with Electron Cyclotron Emission (ECE) measurements. ECE enables the radial localization of the magnetic island quite precisely by the phase jump of the oscillation [1].

When modes with the same toroidal but different poloidal mode numbers are phase locked, they have a common frequency and the local phase relation between the individual modes varies in space. In a tokamak coupled modes are usually observed to rotate as a rigid body in the toroidal direction. Thus, the phase relation varies with the poloidal angle only and observation at a single toroidal position is sufficient.

A (2,1) mode is mostly coupled to a (1,1) core mode when  $q_0 < 1$ , while coupling to ( $m > 2, n = 1$ ) TMs is not a general observation.

Several publications reporting the observed coupling of tearing modes or predicting the phase relation between  $n = 1$  TMs suggest that the modes are in phase on the low field side (LFS). In [2] and [3] this is observed prior to a density limit disruption for the (3,1) and (2,1) TMs. Representing tearing modes by helical perturbation currents, the island O-points are expected to be aligned on the LFS [4]. Recent simulations [5] with the non-linear MHD code JOEAK [6]

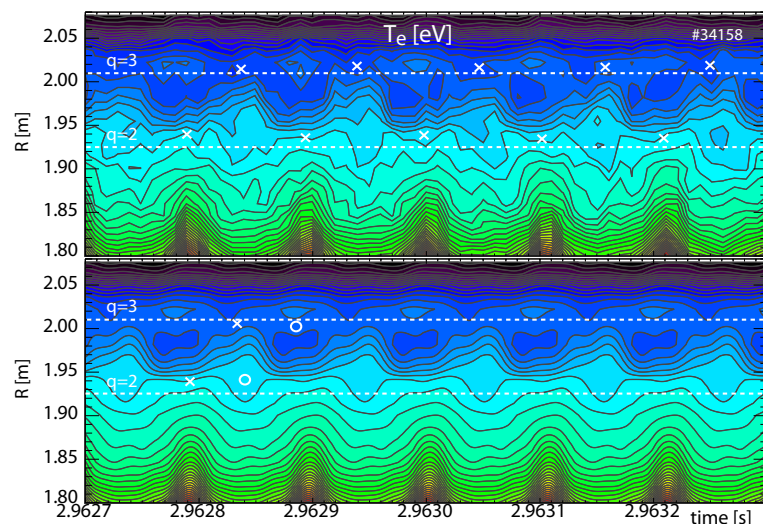


Figure 1: ECE coloured contours showing coupled (2,1) and (3,1) islands. Top: downsampled signals ( $\Delta\Phi_{ECE,ds} \approx 0.80$ ), bottom: FFT-reconstructed signals ( $\Delta\Phi_{ECE,FFT} \approx 0.85$ ). Crosses mark X-points, circles mark O-points. Horizontal dashed lines indicate the positions of  $q = 2$  and  $q = 3$  from equilibrium reconstruction.

for low  $\beta$  and low rotation velocity agree with the previous findings.

**Tools for phase difference determination** On ASDEX Upgrade ECE measures the local electron temperature in a single toroidal location at various positions along a horizontal line approximately at the midplane. The observation regions are mainly on the LFS. Thus, a direct distinction of mode numbers from ECE is not possible. The toroidal mode number,  $n$ , for the mode frequency to be considered, is determined by a toroidally arranged array of Mirnov coils. Local oscillations in the ECE signals can be assigned to poloidal mode numbers,  $m$ , via the  $q$  profile from magnetic equilibrium reconstruction. In order to reduce the noise in the fast (1 MHz) acquired ECE signals we apply two methods. The signals are downsampled to 100 kHz or reconstructed from the FFT spectrum. For the latter, three harmonics of the mode fundamental frequency are considered in order to describe the non-sinusoidal ECE signals in the region of magnetic islands [7]. The FFT method often shows clearer structures and suppresses other modes (unless their frequency matches one of the harmonics) but is applicable only for mode phases that are sufficiently stationary.

For both methods contouring is applied. Figure 1 shows coloured contours for a time interval with coupled (2,1) and (3,1) islands. For the downsampled contour the phase difference on the LFS,  $\Delta\Phi_{ECE,ds}$ , is determined from the averaged temporal shift between island X-points. For the FFT-filtered contour, the phase difference,  $\Delta\Phi_{ECE,FFT}$ , is the average of the shift between X points and O-points, respectively.  $\Delta\Phi_{ECE} \in [0, \pi]$  corresponds to a (3,1) mode lagging behind the (2,1) in the direction of Neutral Beam Injection (NBI) induced toroidal plasma rotation.

An independent method for phase determination relies on magnetic measurements, specifically on a set of poloidally arranged Mirnov coils in one toroidal position. The Mirnov Interpretation Code (MIC) [3] represents a magnetic island by a helical current layer on a resonant surface according to  $j(\rho, \Theta) = j_0 \delta(\rho - \rho_{res}) \cos(m\Theta^*(\Theta) + n\Phi - \omega t + \phi_0)$ . Induced currents in the vessel and in the Passive Stabilization Loop (PSL) are considered for the determination of perturbation fields,  $\tilde{B}_\theta$ , at the Mirnov coil positions. Simulated  $\tilde{B}_\theta$  from single TMs for the respective magnetic equilibrium are determined with MIC. The fit to the measurements, with modes' phases and amplitudes as free parameters, is performed in a separate code. The phase differences between

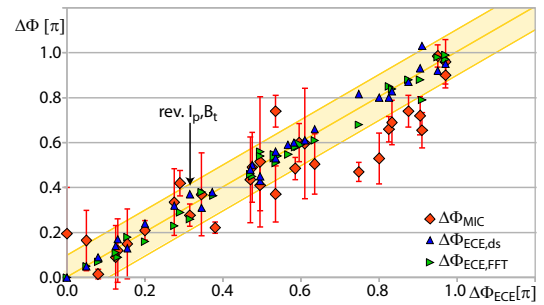


Figure 2:  $\Delta\Phi_{MIC}$ ,  $\Delta\Phi_{ECE,ds}$  and  $\Delta\Phi_{ECE,FFT}$  vs.  $\Delta\Phi_{ECE} = (\Delta\Phi_{ECE,ds} + \Delta\Phi_{ECE,FFT})/2$ , including one case with reversed  $I_p$  and  $B_t$ . The yellow region indicates the estimated uncertainty in  $\Delta\Phi_{ECE}$ . Error bars for  $\Delta\Phi_{MIC}$  indicate only the difference between the results for the two chosen sets of  $m$  numbers.

$m = 2$  and  $m = 3$  modes on the LFS for  $m \in [2, 3]$  and  $m \in [2, 3, 4, 5]$  are averaged to give  $\Delta\Phi_{MIC}$ . Figure 2 shows that  $\Delta\Phi_{MIC}$  and  $\Delta\Phi_{ECE}$  are reasonably consistent and clearly show the same trend. However, the degree of agreement between measurements and simulated coupled modes from MIC is not always satisfactory. Furthermore, the sensitivity of the fit to the coil selection or measurement errors have not yet been determined. This will be investigated further.

**Implications of coupled modes** Figure 2 reveals that (2,1) and (3,1) islands can couple with any phase relation  $\Delta\Phi$  within  $[0, \pi]$ . For phase locked modes the observed mode amplitude and phase in magnetic pick-up coils strongly depend on the poloidal position. Measurements on the LFS only can be misleading and mode detection might fail in case of coupled modes. Figure 3 shows time traces of  $d\tilde{B}_\theta/dt$  at the midplane on LFS and high field side (HFS). In this case  $\Delta\Phi \approx \pi$ , such that the mode amplitudes add up on the HFS while on the LFS the effective amplitude roughly corresponds to the difference. Accordingly, spatially filtered signals for specific toroidal mode numbers should be determined at least for HFS and LFS in order to estimate the correct mode amplitude.

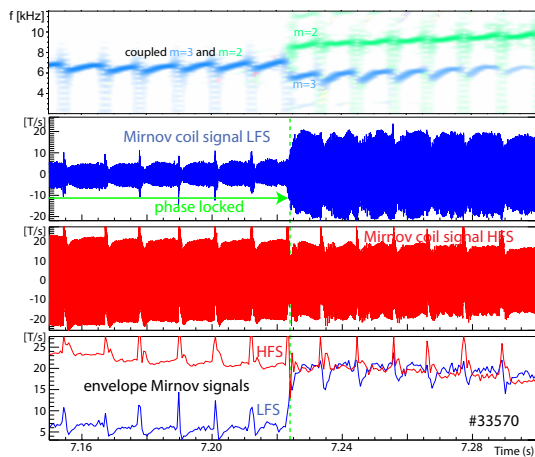


Figure 3:  $m$  number spectrogram (top), Mirnov coil signals at midplane LFS and HFS (middle) and corresponding upper envelope signals (bottom) for a case with  $\Delta\Phi \approx \pi$  up to 7.224 s. From 7.224 s on, the modes are decoupled with separate frequencies, thus the envelope shows the sum of their amplitudes.

Knowledge of the local phase for a specific mode may be important, e.g. for island stabilisation by current drive in the island's O-point using modulated electron cyclotron current drive (ECCD) [8]. In order to determine the correct ECCD timing from magnetic measurements in case of coupled modes, the phase relation between the contributing modes has to be known and considered.

**Dependencies of phase difference** Theoretical considerations of coupled islands up to now consider purely current driven tearing modes in plasmas with low pressure and toroidal rotation velocity [4, 5]. These islands are expected to be in phase on the LFS. One possible reason for islands shifted with respect to this position might be the viscous drag on the islands by the NBI induced fluid rotation. Another contribution might arise from the kink response that can govern the edge displacement [9] and increases with pressure [10].

Nearly all analysed coupled modes rotate in the NBI direction with the plasma rotation frequency at the  $q = 2$  surface being higher than at the  $q = 3$ . The analysed cases with opposite mode rotation have  $\Delta\Phi$  so close to 0 that its sign cannot be reliably determined. All cases

analysed so far have  $\Delta\Phi \in [0, \pi]$ , which means that the (3,1) mode lags behind the (2,1). This hints to the differential plasma rotation as source of the phase shift. Figure 4 shows  $\Delta\Phi_{MIC}$  and  $\Delta\Phi_{ECE}$  as function of the mode frequency,  $f_{n=1}$ , as well as of the normalized plasma beta,  $\beta_N$ . With both parameters the observed phase shifts show an increasing trend.

Although the correlation with  $\beta_N$  appears higher than with  $f_{n=1}$  ( $\Delta\Phi \approx 0.5$  occurs at  $f_{n=1} = 750$  Hz and 13000 Hz), it is clear that neither of these parameters should fully

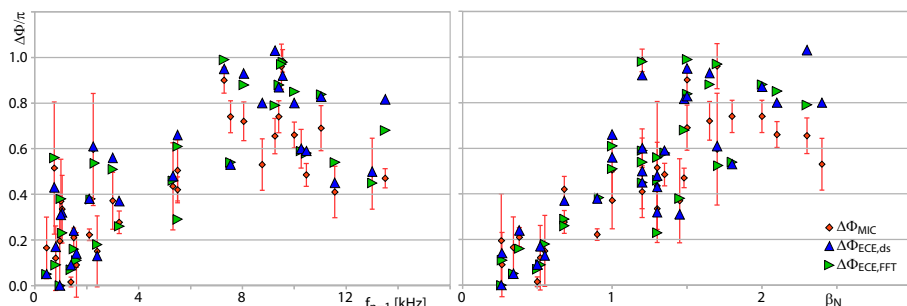


Figure 4:  $\Delta\Phi$  vs. mode frequency  $f_{n=1}$  and vs.  $\beta_N$ .

determine  $\Delta\Phi$ :  $\beta_N$  is

only a global parameter and  $f_{n=1}$  is a weak approximation for the viscous drag on the modes. For a meaningful force balance between friction and attracting forces between the islands' perturbation currents, the required precision of the involved quantities is beyond the experimentally accessible one. However, in one case, a stationary coupled phase with  $0.9\pi < \Delta\Phi < 1.05\pi$  occurs for more than 0.5 s. Should the viscous drag be responsible for the phase shift,  $\Delta\Phi \approx \pi$  would mean that friction and attracting forces are equal in strength. This situation should not be stationary but lead to decoupling of the modes. (The modes in this case decouple without change in  $\Delta\Phi$  but with decreasing mode amplitude.) Simulations with the JOREK code for significant  $\beta_N$  and including externally induced toroidal rotation are planned. With this, disentangling the rotation and pressure contributions with well-defined islands should be possible.

## References

- [1] M. Reich et al, Fusion Science and Technology **61**, 309 (2012)
- [2] W. Suttrop et al, Nucl. Fusion **37**, 119 (1997)
- [3] M. Schittenhelm, H. Zohm and ASDEX Upgrade Team, Nucl. Fusion **37**, 1255 (1997)
- [4] S. Yoshimura et al, Physics of Plasmas **9**, 3378 (2002) (and references therein)
- [5] F. Wieschollek, M. Hölzl, private communication (06/2019)
- [6] G.T.A. Huysmans, O. Czarny, Nucl. Fusion **47**, 659 (2007)
- [7] V. Igochine et al, Physics of Plasmas **21**, 110702 (2014)
- [8] W. Kasperek et al, Nucl. Fusion **56**, 126001 (2016) (and references therein)
- [9] B. Tobias et al, Plasma Phys. Control. Fusion **55**, 095006 (2013)
- [10] P. Piovesan et al, Plasma Phys. Control. Fusion **59**, 014027 (2017)

This work has been carried out within the framework of the EUROfusion Consortium and has received funding from the Euratom research and training programme 2014-2018 and 2019-2020 under grant agreement No 633053. The views and opinions expressed herein do not necessarily reflect those of the European Commission.